1.0

4.5
5.0
5.9

2.8

2.5

1.1

3.2

2.2

3.6

4.0

2.0

1.8

1.25

1.4

1.6

MICROCOPY RESOLUTION TEST CHART

NATIONAL BUREAU OF STANDARDS-1963-A

AUSTRALIA

DEPARTMENT OF DEFENCE

DEFENCE SCIENCE AND TECHNOLOGY ORGANISATION

WEAPONS RESEARCH ESTABLISHMENT

SALISBURY, SOUTH AUSTRALIA

TECHNICAL REPORT 1858 (W)

SUBSONIC, INVISCID FLOW BY THE FINITE ELEMENT METHOD

C.A.J. FLETCHER

DDC
RECEIVED
MAR 24 1978
D

Approved for Public Release.

UNCLASSIFIED
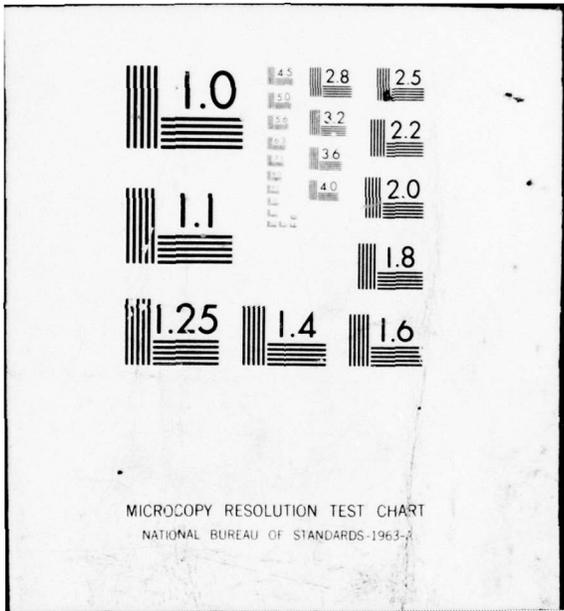
AR-000-933

DEPARTMENT OF DEFENCE

DEFENCE SCIENCE AND TECHNOLOGY ORGANISATION

WEAPONS RESEARCH ESTABLISHMENT

TECHNICAL REPORT 1858 (W)

SUBSONIC, INVISCID FLOW BY THE FINITE ELEMENT METHOD

C.A.J. Fletcher

Aug 77

40 P.

WRE-TR-1858(W)

S U M M A R Y

Galerkin and least-squares finite element formulations in terms of the primitive variables have been applied to the equations governing compressible, inviscid flow. A novel finite element representation for the groups of variables, rather than the single variables, occurring linearly in the conservation form of the governing equations has led to a relatively sparse stiffness matrix. The Galerkin formulation was used in conjunction with Newton's method but solutions for the flow about circular cylinders could only be obtained with freestream Mach numbers less than 0.32. The least-squares formulation was applied in conjunction with an iterative scheme of the successive over-relaxation type. Solutions have been obtained for the flow about circular and elliptic cylinders, a 6% circular-arc aerofoil and a NACA-0012 aerofoil at zero angle of attack, with the free-stream Mach number sufficiently large that locally sonic conditions have occurred. The solutions are in good agreement with both experimental results and other computational solutions.

Approved for Public Release

D D C
RECEIVED
MAR 24 1978
D

UNCLASSIFIED

371 700   JOB

DOCUMENT CONTROL DATA SHEET

Security classification of this page   UNCLASSIFIED

1	DOCUMENT NUMBERS	2	SECURITY CLASSIFICATION
AR Number: AR-000-933		a. Complete Document:	Unclassified
Report Number: WRE-TR-1858(W)		b. Title in Isolation:	Unclassified
Other Numbers:		c. Summary in Isolation:	Unclassified

3	TITLE
	SUBSONIC, INVISCID FLOW BY THE FINITE ELEMENT METHOD

4	PERSONAL AUTHOR(S):	5	DOCUMENT DATE:
	C.A.J. Fletcher		August 1977

6	6.1	TOTAL NUMBER OF PAGES	43
	6.2	NUMBER OF REFERENCES:	26

7	7.1 CORPORATE AUTHOR(S):	8	REFERENCE NUMBERS
	Weapons Research Establishment		a. Task: DST 76/009
			b. Sponsoring Agency:
	7.2 DOCUMENT (WING) SERIES AND NUMBER	9	COST CODE:
	Weapons Research and Development Wing TR-1858		331202/343

10	IMPRINT (Publishing establishment):	11	COMPUTER PROGRAM(S) (Title(s) and language(s))
	Weapons Research Establishment		

12	RELEASE LIMITATIONS (of the document):
	Approved for Public Release

12.0	OVERSEAS	NO	P.R.	1	A	B	C	D	E

Security classification of this page: UNCLASSIFIED

| 13 | ANNOUNCEMENT LIMITATIONS (of the information on these pages): |

No limitation

| 14 | DESCRIPTORS: | | 15 | COSATI CODES: |

a. EJC Thesaurus Terms

Subsonic flow   Cylindrical bodies
Least-squares method   Airfoils
Inviscid flow   Equations of motion
Compressible flow

2004
1201

b. Non-Thesaurus Terms

Finite element method
Galerkin
Newton's method
NACA-0012 airfoil

| 16 | LIBRARY LOCATION CODES (for libraries listed in the distribution): |

SW   SR   SD   AACA   NL

| 17 | SUMMARY OR ABSTRACT:
(if this is security classified, the announcement of this report will be similarly classified)

    Galerkin and least-squares finite element formulations in terms of the
primitive variables have been applied to the equations governing
compressible, inviscid flow.   A novel finite element representation for
the groups of variables, rather than the single variables, occurring
linearly in the conservation form of the governing equations has led to a
relatively sparse stiffness matrix.   The Galerkin formulation was used in
conjunction with Newton's method but solutions for the flow about circular
cylinders could only be obtained with freestream Mach numbers less than
0.32.   The least-squares formulation was applied in conjunction with an
iterative scheme of the successive over-relaxation type.   Solutions have
been obtained for the flow about circular and elliptic cylinders, a 6%
circular-arc aerofoil and a NACA-0012 aerofoil at zero angle of attack,
with the free-stream Mach number sufficiently large that locally sonic
conditions have occurred.   The solutions are in good agreement with both
experimental results and other computational solutions.

TABLE OF CONTENTS

LIST OF APPENDICES

LIST OF FIGURES

1.   INTRODUCTION

The purpose of this report is to examine a number of different finite element formulations suitable for external, inviscid, subcritical flow.   As such it is a stepping-stone towards the treatment of transonic, external, inviscid flow. Most previous finite element applications to subcritical flow e.g.(ref.1,2,3) have been based on either a velocity potential or stream function formulation. However no formulation based on the full equations of motion has been successful in obtaining solutions that contained significant regions of embedded supersonic flow.   For this and other reasons set out in Section 2, the present formulation makes direct use of the primitive variables, i.e. velocity, density and pressure.   It is believed that this is the first time a primitive variable finite element formulation has been applied to the full equations of motion governing compressible, inviscid flow.

In order to ensure an efficient finite element algorithm it is important to establish consistent analytic representations for each of the dependent variables; this problem is considered in Section 2.   For problems that do not possess a variational formulation the two most effective finite element methods are based on the Galerkin and least-squares formulations.   Both these formulations have been applied to the current problem and reduction of the governing partial differential equations to algebraic equations is described in Section 2.

The governing equations, in both the differential and algebraic form, are highly nonlinear and require iterative solution techniques;   these are described in Section 3.   A modified Newton's method has been used in conjunction with the Galerkin formulation.   Because Newton's method will only converge for a starting solution relatively close to the final solution it has been necessary to use an ancilliary technique to get close to the final solution.   This has been achieved by utilising the unsteady version of the governing equations.   After application of the finite element formulation, these equations have been treated as ordinary differential equations in time and have been integrated until the converged solution is approached.   Because the least-squares formulation leads to a positive-definite stiffness matrix it has been possible to apply a successive over-relaxation (SOR) method of solution after locally linearising the algebraic equations.

Solutions for the flow about circular and elliptic cylinders using both the Galerkin and least-squares formulations are given in Section 4.   Solutions for the flow about two representative aerofoils at various free-stream Mach numbers are presented in Section 5.   Comparisons are made with experimental results and with other computational results.   A comparison of the Galerkin and least-squares formulations as applied to the current problem is made in Section 6.

2.   FORMULATION OF THE PROBLEM

In Section 2.1 the relative merits of the velocity potential and primitive variable formulations applied to subcritical, inviscid flow are presented. The equations of motion appropriate to both steady and unsteady flow and the corresponding boundary conditions are indicated in Section 2.2.   Different orders of analytic representation for different variables are possible and these are discussed.   Both the Galerkin and least-squares finite element formulations have been used to reduce the governing partial differential equations to algebraic equations;   these are described in Sections 2.3 and 2.4 respectively.

2.1 Velocity potential vs. primitive variables

A velocity potential formulation of subcritical, inviscid flow might express the governing equations in terms of the velocity potential, φ and the local sound speed, a.   In two dimensions the governing equations are

$$(a^2 - \varphi_x^2) \cdot \varphi_{xx} - 2\varphi_x \cdot \varphi_y \cdot \varphi_{xy} + (a^2 - \varphi_y^2) \cdot \varphi_{yy} = 0 \tag{1}$$

and

$$a^2 + \frac{\gamma - 1}{2} \cdot (\varphi_x^2 + \varphi_y^2) = a_o^2. \tag{2}$$

In equations (1) and (2) γ is the specific heat ratio and a_o is the stagnation value of the sound speed. The use of equations (1) and (2) is attractive because only one unknown, $\overline{\varphi}$, is required at each node. Equation (2) is treated as a local algebraic relationship which adjusts the value of 'a' at each step of the iteration.

Equation (1) can be written as a Poisson-like equation

$$\varphi_{xx} + \varphi_{yy} = f, \tag{3}$$

in which f incorporates all the terms associated with the compressible nature of the flow. Application of a variational finite element formulation of equation (3) permits an iterative solution in which f is recalculated after each solution for φ. The iterative procedure fails at a local Mach number of unity(ref.2,3). This is probably due to the use of equation (2) to adjust the value of 'a'. It is interesting that a linearisation of equation (1) that leads to the transonic small perturbation equation and avoids the use of equation (2) can be iterated to locally supersonic Mach numbers(ref.4).

Another disadvantage of the use of equations (1) and (2) is that the converged solution, φ must be differentiated numerically before a useful quantity, the pressure at the body surface, can be obtained. Also since equation (1) is highly nonlinear, application of a finite element formulation results in a large number of cross-terms that must be manipulated at each step of the iterative process. This results in a considerable increase in computation time.

To avoid some of the disadvantages noted above the present formulation makes use of the primitive variables and expresses the governing equations in conservation form:

$$(\rho u)_x + (\rho v)_y = 0, \tag{4}$$

$$(\rho u^2 + p)_x + (\rho uv)_y = 0, \tag{5}$$

$$(\rho uv)_x + (\rho v^2 + p)_y = 0, \tag{6}$$

$$p = k \cdot \rho^\gamma. \tag{7}$$

Equations (4) to (6) all have the same structure and are linear in the groups of variables. In the present formulation advantage is taken of these features to reduce substantially the number of cross-terms that appear. Equations (4) to (6) and the energy equation,

$$\frac{\gamma p}{(\gamma - 1)\rho} + \tfrac{1}{2}(u^2 + v^2) = \frac{\gamma}{(\gamma - 1)}\frac{p_\infty}{\rho_\infty}, \tag{8}$$

have been found to be suitable for solving flow problems at low to inter-
mediate free-stream Mach numbers. The primitive variable formulation gives
the required final solution, the pressure on the body, directly. A dis-
advantage of the primitive variable formulation is that three unknowns per
node are required.

2.2 Equations of motion and finite element representation

Because of the technique used to provide starting data for the Galerkin
formulation (Section 3.3) the unsteady, compressible, inviscid equations will
be presented. Following Peyret and Viviand(ref.5) the conservation form of
the governing equations is

$$\frac{\partial W}{\partial t} + \frac{\partial F}{\partial x} + \frac{\partial G}{\partial y} = 0, \tag{9}$$

where W, F and G are three component vectors

$$W = \begin{bmatrix} \rho u \\ \rho v \\ \rho \end{bmatrix}, \; F = \begin{bmatrix} \rho u^2 + p \\ \rho uv \\ \rho u \end{bmatrix}, \; G = \begin{bmatrix} \rho uv \\ \rho v^2 + p \\ \rho v \end{bmatrix}. \tag{10}$$

Equations (4) to (6) are equivalent to

$$\frac{\partial F}{\partial x} + \frac{\partial G}{\partial y} = 0. \tag{11}$$

To stabilise the integration of the unsteady equations (Section 3.3) the
following related equations will also be considered,

$$\frac{\partial W}{\partial t} + \frac{\partial F}{\partial x} + \frac{\partial G}{\partial y} = a\left\{ \frac{\partial^2 W}{\partial x^2} + \frac{\partial^2 W}{\partial y^2} \right\}. \tag{12}$$

The coefficients a, in equation (12), are chosen to be as small as possible
consistent with the convergence of the integration of the unsteady equations.
Equations (4) to (12) are non-dimensionalised by defining

$$u_{nd} = u/U_\infty, \; v_{nd} = v/U_\infty, \; \rho_{nd} = \rho/\rho_\infty \text{ and } p_{nd} = (p - p_\infty)/\rho_\infty U_\infty^2. \tag{13}$$

The resultant form of equations (12) remains unaltered if a new t and a are
defined. From now on the subscript nd will be dropped. Equation (7)
becomes

$$1 + \gamma . M_\infty^2 . p = \rho^\gamma \tag{14}$$

and equation (8), with some rearrangement, becomes

$$1 + \gamma . M_\infty^2 . p = \rho\left\{ 1 + \frac{\gamma - 1}{2} . M_\infty^2 . \left[1 - (u^2 + v^2) \right] \right\}. \tag{15}$$

In this report either equation (14) or (15) has been used to link p to the
other variables.

The far-field boundary conditions are applied at a finite distance from the body in the form

$$u = u_{fs}$$
$$v = v_{fs} \tag{16}$$
$$\rho = \rho_{fs}.$$

Two choices for the far-field boundary conditions have been considered. Firstly $u_{fs} = 1.0$, $v_{fs} = 0$, $\rho_{fs} = 1.0$. Secondly a Prandtl-Glauert transformation has been applied and the distorted body shape has been used. For the flow about circular cylinders and ellipses the far-field velocity components have been calculated from a complex variable solution of the distorted body. For the flow about aerofoils, thin-aerofoil theory has been applied to the distorted body (see Appendix I). Once the velocity components are available equations (14) and (15) have been used to give the density. Complex variable theory and thin aerofoil theory have also been used to give starting data throughout the flow-field.

The boundary condition at the body has required that the flow is locally tangential to the body surface. This has given a relationship between $\bar{u}_j$ and $\bar{v}_j$ and $(\bar{\rho u})_j$ and $(\bar{\rho v})_j$ at the nodes on the body.

As the first step of the finite element formulation analytic representations for the dependent variables are introduced. In the present report these are introduced for the groups of variables W, F and G in equation (10). E.g.

$$\rho u = \sum_j N_j(x,y) \cdot (\bar{\rho u})_j, \tag{17}$$

where N_j is the shape function appropriate to the jth node and $^-$ indicates the nodal value of the different variables. It is believed that this is the first finite element formulation in which groups of variables, rather than single variables, have been given an analytic representation. This technique has been used Previously(ref.6,7) in the application of an Orthonormal Method of Integral Relations to supersonic boundary-layer flow. An immediate advantage of finite element representations like equation (17) is that, since the governing equations are linear in the groups of variables, only single summations occur after application of the finite element method. Thus the computation of the equation residuals can be accomplished more efficiently.

One difficulty associated with the finite element method applied to a system of equations, like (11) and (12), is to ensure that the orders of the shape functions that appear in the analytic representations like equation (17) are chosen consistently. If the Galerkin formulation is used then the corresponding choice of the order of the weight functions presents similar difficulties. Failure to choose the orders of the shape functions consistently produces a less efficient solution i.e. more nodal unknowns and a more refined grid will be required to achieve comparable accuracy.

Taylor and Hood(ref.8), after applying a Galerkin finite element formulation to slow viscous flow, concluded that for consistency:

(i) the maximum order of error associated with the residual of each variable must be equal

(ii) The residuals arising from each equation must be weighted according to the maximum error occurring in each equation.

It is well-known that for slow viscous flow the momentum equations are dominated by the pressure gradient and viscous dissipation terms whereas the convective or inertia terms are of smaller magnitude.   However for high speed flows the momentum equations are dominated by the balance between the inertia terms and the pressure gradient terms;   the viscous terms only become significant where a large velocity gradient occurs e.g. adjacent to a surface. Thus it would seem desirable to replace (i) with the condition that

> (iii) the order of the representation of the flow variables should produce errors consistent with the physical processes being modelled.

For the case of slow viscous flow condition (iii) leads to a first order representation for p and a second order representation for u, v.

Equations (4) to (6) could be applied to incompressible, inviscid flow. In this case ρ is constant.   On physical grounds it would be expected that all groups of variables in each equation would be of the same order of magnitude.   Since only first derivatives appear each group of variables in each equation will require the same order of representation to satisfy condition (iii).

Thus

$$X = \sum_{j} L_j(x,y) \cdot \overline{X}_j \tag{18}$$

where

$$X = (\rho u, \rho v)$$

and

$$Y = \sum_{j} M_j(x,y) \cdot \overline{Y}_j, \tag{19}$$

where $Y = (\rho u^2, \rho uv, \rho v^2, p)$. L_j and M_j are shape functions of, as yet, undetermined orders.   Suppose u, v are represented by n^{th} order shape functions i.e.

$$u \sim x^n$$

then

$$\rho u \sim x^n$$

and

$$p \sim \rho u^2 \sim x^{2n}.$$

Thus the lowest consistent representation would be for L to be first order and M to be second order, i.e.

$$\frac{O(M_j)}{O(L_j)} = 2.$$

(20)

In contrast to slow viscous flow, inviscid incompressible flow requires a first order representation for u and v and a second order representation for p.

If equations (4) to (6) are applied to compressible, inviscid flow representations (18) and (19) are also applicable.   In this case

$$p \sim \rho^\gamma$$

therefore

$$\rho^{\gamma-1} \sim u^2$$

and if

$$u \sim x^n$$

$$\rho \sim x^{\frac{2n}{\gamma - 1}}$$

$$\rho u \sim x^{(\frac{\gamma + 1}{\gamma - 1}) n}$$

and

$$p \sim \rho u^2 \sim x^{(\frac{2\gamma}{\gamma - 1}) n}$$

and

$$\frac{O(M_j)}{O(L_j)} = \frac{2\gamma}{\gamma + 1}.$$

(21)

Since only integral order representations are possible the lowest, consistent representation, with $\gamma = 1.4$, would have L_j as a sixth order shape function and M_j as a seventh order shape function.   If a Galerkin formulation were employed seventh and sixth order shape functions weighting the continuity and momentum equations respectively would also be required.   Clearly such a high-order representation would be unwieldy and possibly, because of the relatively dense stiffness matrix, be inefficient.

If compressible, inviscid flow is to be represented by a moderately low order system, equation (21) suggests that L_j and M_j should be of the same order.   Consequently, based on the results of reference 9 all groups of variables have been represented by quadratic shape functions of the Serendipity family in rectangular isoparametric elements.

2.3 The Galerkin finite element formulation

The Galerkin method may be written as

$$\iint N_i \cdot R^{(k)} \cdot dx\ dy = 0, \quad k = 1, 3; \quad i = 1, n \tag{22}$$

where N_i is the shape function appropriate to the ith node and $R^{(k)}$ is the equation residual after substitution of analytic representations like equation (17). For the present problem the Galerkin formulation follows reference 10. After application of the Galerkin formulation equation (11) becomes

$$\sum_j s_{ij} \cdot \frac{\partial \overline{W}_j}{\partial t} + \sum_j a_{ij} \cdot \overline{F}_j + \sum_j b_{ij} \cdot \overline{G}_j = a \sum_j c_{ij} \cdot \overline{W}_j, \quad i = 1, n$$

$$\tag{23}$$

where

$$s_{ij} = \iint N_i \cdot N_j\ dx\ dy,$$

$$a_{ij} = \iint N_i \cdot \frac{\partial N_j}{\partial x} \cdot dx\ dy,$$

$$= \iint N_i \cdot \frac{\partial N_j}{\partial y} \cdot dx\ dy, \tag{24}$$

and

$$c_{ij} = \int \left\{ N_i \cdot \frac{\partial N_j}{\partial x} \cdot dy - \frac{\partial N_j}{\partial y} \cdot dx \right\}$$

$$- \iint \left\{ \frac{\partial N_i}{\partial x} \cdot \frac{\partial N_j}{\partial x} + \frac{\partial N_i}{\partial y} \cdot \frac{\partial N_j}{\partial y} \right\} dx\ dy.$$

$\overline{W}_j$ etc. are the values of W etc., given by equation (12), at the jth node.

The coefficients s_{ij}, a_{ij}, b_{ij} and c_{ij} are evaluated for each ith node after introducing an isoparametric formulation(ref.9). s_{ij}, a_{ij} and b_{ij} can be obtained from intermediate coefficients that are evaluated, once and for all, on a dummy element(ref.9). a_{ij} and b_{ij} are the same expressions as arise in the treatment of inviscid, incompressible flow(ref.9).

2.4 Least-squares finite element formulation

The least-squares formulation presented here follows that of Zienkiewicz, Owen and Lee(ref.11). Substitution of the analytic representation, equation (17), into the governing equations (4) to (6), produces residuals of the following form in each element:

$$R^{(1)} = \sum_j \frac{\partial N_j}{\partial x} \cdot (\overline{\rho u})_j + \sum_j \frac{\partial N_j}{\partial y} \cdot (\overline{\rho v})_j, \tag{25}$$

$$R^{(2)} = \sum_j \frac{\partial N_j}{\partial x} \cdot (\overline{\rho u^2} + \overline{p})_j + \sum_j \frac{\partial N_j}{\partial y} \cdot (\overline{\rho uv})_j, \tag{26}$$

$$R^{(3)} = \sum_j \frac{\partial N_j}{\partial x} \cdot (\overline{\rho uv})_j + \sum_j \frac{\partial N_j}{\partial y} \cdot (\overline{\rho v^2} + \overline{p})_j. \tag{27}$$

The least-squares formulation requires that

$$\iint (a_1 \cdot R^{(1)2} + a_2 \cdot R^{(2)2} + a_3 \cdot R^{(3)2}) \, dx \, dy = \text{minimum}, \tag{28}$$

where a_1, a_2 and a_3 are scalars that may be used to adjust the weight of the various equations. Differentiating equation (28) with respect to each of the unknown nodal values in turn produces the following result:-

$$\iint \left\{ a_1 \cdot \frac{\partial R^{(1)}}{\partial \overline{q}_i} \cdot R^{(1)} + a_2 \cdot \frac{\partial R^{(2)}}{\partial \overline{q}_i} \cdot R^{(2)} + a_3 \cdot \frac{\partial R^{(3)}}{\partial \overline{q}_i} \cdot R^{(3)} \right\} dx. dy = 0, \quad i = 1, n \tag{29}$$

where $\overline{q}_i = \{(\overline{\rho u})_i, (\overline{\rho v})_i, \overline{\rho}_i\}$. Substitution of equations (25) to (27) into equations (29) and evaluation of the integrals, produces the following algebraic equations:

$$S_i^{(m)} = \sum_j \left\{ r_{ij}^{(m)} \cdot (\overline{\rho u})_j + s_{ij}^{(m)} \cdot (\overline{\rho v})_j + t_{ij}^{(m)} \cdot (\overline{\rho u^2})_j + x_{ij}^{(m)} \cdot (\overline{\rho uv})_j + \right.$$

$$\left. y_{ij}^{(m)} \cdot (\overline{\rho v^2})_j + z_{ij}^{(m)} \cdot \overline{p}_j \right\} = 0, \quad m = 1, 3; \quad i = 1, n. \tag{30}$$

In equation (30) $m = 1$ corresponds to $\overline{q}_i = (\overline{\rho u})_i$ in equation (29). Thus three equations are formed at each node if there are three unknown nodal values. In equation (30) $r_{ij}^{(m)}$ etc. are algebraic functions of a_{ij}, b_{ij}, c_{ij}, d_{ij}, $\overline{\rho u}_i$, $\overline{\rho v}_i$ and $\overline{\rho}_i$ where

$$\left. \begin{aligned}
a_{ij} &= \iint \frac{\partial N_i}{\partial x} \cdot \frac{\partial N_j}{\partial x} \, dx \, dy, \\[2ex]
b_{ij} &= \iint \frac{\partial N_i}{\partial y} \cdot \frac{\partial N_j}{\partial y} \cdot dx \, dy, \\[2ex]
c_{ij} &= \iint \frac{\partial N_i}{\partial x} \cdot \frac{\partial N_j}{\partial y} \cdot dx \, dy, \\[2ex]
d_{ij} &= \iint \frac{\partial N_i}{\partial y} \cdot \frac{\partial N_j}{\partial x} \cdot dx \, dy.
\end{aligned} \right\} \tag{31}$$

Equations (31) may be compared with equations (24) which arise through application of the Galerkin formulation. Once isoparametric elements are introduced(ref.9), equations (31) are considerably more complicated and time-consuming to evaluate than equations (24). The algebraic expressions for $r_{ij}^{(m)}$ etc. depend on whether equation (14) or (15) is used to obtain p as a function of the other variables. The detailed expressions are given in Appendix II.

3. ITERATIVE SOLUTION TECHNIQUES

The main difficulty, associated with solving either equations (23) that arise from the Galerkin formulation or equations (30) that arise from the least-squares formulation, is that the nodal unknowns $\overline{\rho u}_j$, $\overline{\rho v}_j$ and $\overline{\rho}_j$ occur nonlinearly. Groups of terms, like $\overline{\rho uv}_j$, are interpreted as $(\overline{\rho u}_j \cdot \overline{\rho v}_j)/\overline{\rho}_j$.

Newton's method (Section 3.1) was used initially to solve the steady version of equations (23) in the form

$$\sum_j a_{ij} \cdot \overline{F}_j + \sum_j b_{ij} \cdot \overline{G}_j = 0, \ i = 1,n. \tag{32}$$

However this produced a singular Jacobian. This problem was overcome by differentiating the energy equation (15) with respect to x and y and using these equations instead of the x-momentum equation on the y-axis of symmetry and instead of both momentum equations at the body surface.

In practice it was found that the inversion of the Jacobian required large amounts of main storage and large execution time even after introduction of the sparse matrix techniques described in reference 9. In order to make Newton's method more efficient various modifications were made and these are described in Section 3.2. As the number of nodal unknowns in the flow field was increased difficulty occurred in obtaining starting solutions that were sufficiently close to the converged solution to permit convergence of Newton's method. This result

is consistent with the findings of reference 12.

To alleviate the situation the governing equations in unsteady form (23) were integrated as though they were simultaneous ordinary differential equations in time.   This was a fairly slow process and was terminated as soon as the iterative solution was close enough to the final solution to permit Newton's method to converge.   A description is given in Section 3.3.   Because the least-squares formulation leads to a positive-definite stiffness matrix it is possible to use an SOR-type iterative scheme to solve equations (30).   This is described in Section 3.4.

3.1 Newton's method

This will be described in relation to the solution of equation (32) which can be written as

$$R_i(\overline{q}) = 0, \ i = 1,n, \tag{33}$$

where $\overline{q}$ is a vector of all the nodal unknowns $\overline{w}_j$, equation (10), and R_i represents the residual of the ith equation.   If an arbitrary starting solution, $\overline{q}_o$, is substituted into equation (32) non-zero equation residuals result.   In the neighbourhood of $\overline{q}_o$ the solution can be obtained by application of a Taylor series expansion.

$$\overline{R}_1 = \overline{R}_o + \frac{\partial \overline{R}}{\partial \overline{q}}(\overline{q}_o) \cdot (\overline{q}_1 - \overline{q}_o) \ \cdots \tag{34}$$

If the Taylor series is truncated as shown and if it is assumed that $\overline{q}_1$ is the exact solution then $R_1 = 0$ and

$$\overline{q}_1 = \overline{q}_o - J^{-1}(\overline{q}_o) \cdot \overline{R}_o, \tag{35}$$

where J is the Jacobian, $\partial\overline{R}/\partial\overline{q}$.   If equation (35) is interpreted as one step of an iteration Newton's method is obtained:

$$\overline{q}_{\nu+1} = \overline{q}_\nu - J_\nu^{-1} \cdot \overline{R}_\nu. \tag{36}$$

The effectiveness of Newton's method depends on the accuracy of the assumptions underlying equations (34) and (35).   Clearly if the starting solution is close to the converged solution the assumptions are reasonable and Newton's method is convergent; close to the converged solution the method has the property of quadratic convergence(ref.13).   A discussion of Newton's method and some iterative techniques based on Newton's method are given in reference 14.

3.2 Modified Newton's method

In practical applications most of the execution time is spent factoring J_ν to form J_ν^{-1} even if sparse matrix techniques and the storage of J_ν^{-1} in factored form are used.   Typically, in early applications of the Galerkin formulation to the present problem, the factorisation of the Jacobian accounted for 80 to 90% of the execution time.   Any modification that permits more utilisation of each evaluation of J_ν^{-1} is clearly desirable.

An obvious modification is to compute p steps with the same J_o i.e.

$$\bar{q}_{\nu+1} = \bar{q}_{\nu} - J_{o}^{-1} \cdot \bar{R}_{\nu} \quad 0 \leqslant \nu \leqslant p - 1. \tag{37}$$

Another improvement can be obtained if $J_{o}^{-1} \bar{R}_{\nu}$ is treated as a vector $\bar{\delta}_{\nu}$ which is small compared with $\bar{q}_{\nu}$. Then $\bar{\delta}_{\nu}$ may be interpreted as a search direction. A series of residuals $\bar{R}_{\nu}^{k}$ are evaluated for various λ_{k} corresponding to $\bar{q}_{\nu+1}^{k}$ given by

$$\bar{q}_{\nu+1}^{k} = \bar{q}_{\nu} - \lambda_{k} \cdot \bar{\delta}_{\nu}. \tag{38}$$

λ_{k} is a scalar and typically takes values between 0 and 2. If $\bar{R}_{\nu}^{o}$ corresponds to the solution $\bar{q}_{\nu}$ i.e. $\lambda_{o} = 0$, then two additional solutions, $\bar{R}_{\nu}^{1}$ and $\bar{R}_{\nu}^{2}$ are obtained corresponding to λ_{1}, λ_{2}. For each solution the global sum of all the residuals, F_{ν}^{k}, is computed from

$$F_{\nu}^{k} = \sum_{i} [R_{i\nu}^{k}]^{2} \tag{39}$$

A quadratic dependence of F_{ν}^{k} on λ_{k} is extracted and the value λ_{min}, which minimises F_{ν} is used to obtain $\bar{q}_{\nu+1}$. The technique of finding a minimum in a particular search direction has been used previously for minimising a sum of squares(ref.15).

Another modification to equation (36) is possible by attempting to approximate J_{ν}^{-1}. Assuming that J_{ν} is close to J_{o}, let

$$J_{\nu} = J_{o} + \gamma. \tag{40}$$

If a first approximation to $\bar{\delta}_{\nu}$ is computed as

$$\bar{\delta}_{\nu}* = J_{o}^{-1} \bar{R}_{\nu}, \tag{41}$$

then a better approximation is

$$\bar{\delta}_{\nu}^{-} = J_{\nu_{a}}^{-1} \bar{R}_{\nu}, \tag{42}$$

where $J_{\nu_{a}}^{-1}$ is an approximation to J_{ν}^{-1}. From equation (40)

$$J_{\nu} = J_{o}(I + J_{o}^{-1} \gamma)$$

and

$$J_{\nu}^{-1} = (I + J_{o}^{-1} \cdot \gamma)^{-1} \cdot J_{o}^{-1}. \tag{43}$$

Equation (43) can be approximated by

$$J_{\nu_a}^{-1} = (I - J_o^{-1} \gamma) \cdot J_o^{-1}.$$

Substitution into equation (42) gives

$$\overline{\delta}_\nu = (I - J_o^{-1} \cdot \gamma) \cdot J_o^{-1} \cdot \overline{R}_\nu$$

or

$$\overline{\delta}_\nu = (I - J_o^{-1} \cdot \gamma) \cdot \overline{\delta}_\nu*.$$

Substitution for γ and simplification gives

$$\overline{\delta}_\nu = \overline{\delta}_\nu* - J_o^{-1}(J_\nu - J_o) \cdot \overline{\delta}_\nu*$$

$$= 2\overline{\delta}_\nu* - J_o^{-1} \cdot J_\nu \cdot \overline{\delta}_\nu*. \tag{44}$$

The modified Newton's method used in the present study has consisted of the following steps:

(i) compute J_o and J_o^{-1}

(ii) use equation (42) to compute $\overline{\delta}_o$

(iii) find a minimum F_o in the $\overline{\delta}_o$ direction

(iv) compute $\overline{q}_\nu$, J_ν

(v) use equation (41) to compute $\overline{\delta}_\nu*$

(vi) use equation (44) to compute $\overline{\delta}_\nu$

(vii) compute a minimum F_ν in the $\overline{\delta}_\nu$ direction

(viii) if F_ν not sufficiently small go to step (iv).

3.3 Starting data for Newton's method

Equation (23) can be rewritten as

$$\sum_j s_{ij} \cdot \frac{\partial \overline{W}_j}{\partial t} = - R_i, \quad i = 1, n \tag{45}$$

where

$$R_i = \sum_j a_{ij} \cdot \overline{F}_j + \sum_j b_{ij} \cdot \overline{G}_j - a \sum_j c_{ij} \cdot \overline{W}_j.$$

In matrix form equation (45) can be inverted to give

$$\dot{W} = - S^{-1} \cdot R. \tag{46}$$

The coefficients of the matrices S only depend on the shape functions and consequently can be inverted once and for all.   To avoid excessive fill-in and to speed up the matrix multiplications on the right hand side of equation (46), matrices like S^{-1} are stored in sparse factored form.

If equations (46) are integrated for large time, the residuals R_i approach zero and consequently the time derivatives $\dot{W}_i$ also approach zero.   The different R_i approach zero at significantly different rates and this causes difficulties for the efficient use of the integration routine.   Gear(ref.16) has produced a predictor/corrector algorithm to suit this situation.   In addition Gear's algorithm automatically adjusts the step-size and the order of the predictor/corrector formula to minimise the integration error.

The term on the right hand side of equation (23) has been introduced to stabilise the numerical integration of equations (46).   Although the additional terms have some physical basis(ref.5) for the momentum equations there is no such basis for the continuity equations.   Therefore it is desirable that a should be as small as possible consistent with convergence.

By expanding equation (46) as a Taylor series about a starting solution $\bar{q}_o$ it is possible to carry out an eigenvalue analysis to determine the critical value of a, below which the integration of equation (46) is unstable. The critical value was found to be approximately $a = 0.1$, and this was confirmed in actual computations.

3.4 One step SOR-Newton's method

Application of the least-squares finite element formulation (Section 2.4) produces a positive definite stiffness matrix.   Consequently an SOR-type solution technique is possible.   This may be obtained by considering a small change in $S_i^{(m)}$ (equation (30)) due to a small change in q_i, where q_i is either $\overline{\rho u}_i$, $\overline{\rho v}_i$, $\bar{\rho}_i$.

$$S_i^{(m)} (\bar{q}_o + \Delta q_i) = S_i^{(m)} (\bar{q}_o) + \frac{\partial S_i^{(m)}}{\partial q_i} (\bar{q}_o) \cdot \Delta q_i = 0, \qquad (47)$$

or in a more general form

$$q_i^{\nu+1} = q_i^{\nu} - \lambda \left[\frac{\partial S_i^{(m)} (\bar{q}_o)}{\partial q_i} \right]^{-1} \cdot S_i^{(m)} (\bar{q}_o). \qquad (48)$$

Examination of equation (30) and Appendix II indicates that both terms like $(\rho u^2)_j$ and ν_{ij} etc. are functions of q_i, thus $\partial S_i^{(m)}/\partial q_i$ is algebraicly complicated.   In contrast to the full Newton's method $\partial S_i/\partial q_i$ is a scalar and trivial to invert, thus no excessive demand is made on main storage or computation time.   However the rate of convergence is slower than Newton's method.   A scalar, λ, has been used to increase the rate of convergence. If λ was greater than 1.7 the iterative process diverged.

4.   FLOW ABOUT CIRCULAR AND ELLIPTIC CYLINDERS

Numerical solutions of the flow-field about circular cylinders have been obtained using a Galerkin finite element formulation and a least-squares finite element formulation.   A schematic representation of the grid used to obtain solutions about both circular and elliptic cylinders is shown in figure 1.   The grid system is essentially polar.   An isoparametric formulation(ref.9) has been used to relate this to a cartesian coordinate system.

Two stagnation points exist for the flow about bluff bodies. At the stagnation points the velocity components, u v are zero. In the present formulation the pressure and density at the stagnation points have been considered part of the boundary conditions by assuming a streamline attaches both stagnation points to the freestream. Consequently equations (14) and (15) can be used to give the following stagnation point values for ρ and p,

$$\rho_{sp} = \left\{ 1 + \left(\frac{\gamma - 1}{2} \right) M_\infty^2 \right\}^{1/(\gamma - 1)} \tag{49}$$

and

$$p_{sp} = (\rho_{sp}^\gamma - 1)/\gamma . M_\infty^2. \tag{50}$$

The far-field boundary conditions are obtained by scaling the x-coordinate by the Prandtl-Glauert factor and then computing the far-field velocity components using complex variable theory (Appendix I).

4.1 Circular cylinder

Results are presented in figure 2 for the variation of the surface Mach number with angular location. Results for free-stream Mach numbers 0.1 to 0.3 have been obtained using the Galerkin finite element formulation. These results have been obtained with 91 elements and 465 nodal unknowns spanning the flow-field. It was found that for free-stream Mach numbers greater than 0.32 Newton's method would not converge even when starting from a converged solution at a free-stream Mach number only marginally smaller. The reason for this is not known.

Solutions obtained using the least-squares formulation at freestream Mach numbers of 0.2 and 0.3 are also shown in figure 2. These results were obtained with 91 elements and 829 nodal unknowns spanning the flow-field. It is apparent that, as the free-stream Mach number is increased, the solutions obtained with the Galerkin formulation indicate a significantly greater acceleration of the flow than those obtained with the least-squares formulation.

Results for the flow about a circular cylinder at a free-stream Mach number of 0.4 are presented in figure 3. The finite element solution has been obtained with a least-squares formulation. The results presented for the surface Mach number have been obtained with 91 elements and 829 nodal unknowns spanning the flow-field.

The finite element solution is compared with solutions obtained by the Method of Lines(ref.17) and series solutions presented by Greenspan and Jain(ref.18); the series solutions are due to Imai(ref.19) and Lush and Cherry(ref.20). The solution by the Method of Lines agrees closely with those of references 19 and 20 and, consequently, has not been plotted.

The finite element solution is in reasonable agreement with the other solutions although it underpredicts the other solutions close to the cylinder shoulder point. Since the solutions given by references 19 and 20 have been obtained by a truncated series representation the difference between those solutions and the finite element solution is not considered significant.

4.2 Elliptic cylinder

A least-squares finite element solution for the flow about a 2:1 elliptic cylinder at a free-stream Mach number of 0.5 is shown in figure 4. These results were obtained with 91 elements and 829 nodal unknowns spanning the flow-field. Solutions were also obtained using the Galerkin formulation at free-stream Mach numbers up to 0.3 but convergence did not occur for major axis/minor axis ratios greater than 1.8.

Numerical calculations using the Method of Integral Relations(ref.21) indicate that the flow is just supersonic at the shoulder of the elliptic cylinder for a free-stream Mach number of 0.5.   In contrast the present solutions indicate that the flow is everywhere subcritical.   The present results are compared with solutions obtained by the Method of Lines(ref.17) which are shown in figure 4.   Agreement is quite good although, as with the results in figure 3, the finite element solution slightly underpredicts the surface velocity on the 'plateau'.

5. FLOW ABOUT AEROFOILS

Solutions for the flow-field about two representative aerofoils have been obtained using the least-squares formulation.   The nature of the grids used has been dictated partially by the shape of the aerofoil in question.   A schematic of the grid used for the circular-arc aerofoil is shown in figure 5.   A deliberate attempt has been made to keep elements far removed from the body surface rectangular; all elements outside the region ABCD are rectangular.   This reduces the number of cross-terms and hence the computation time required to manipulate those terms.

The NACA-0012 aerofoil has a forward stagnation point and if the type of grid shown in figure 5 were used gross distortion of the elements adjacent to the forward stagnation point would occur.   Although the isoparametric formulation is successful in mapping rectangular elements onto a non-rectangular region, the quality of the solution obtained is degraded if the elements become distorted. A schematic of the grid used to obtain flow-field solutions about the NACA-0012 aerofoil is shown in figure 6.   All elements inside the area ABCDEF are rectangular.

A comparison of the grids shown in figures 1, 5 and 6 indicates that basically two types of grid have been used depending on the local body geometry.   Where the body shape can be locally approximated by the arc of a circle a polar grid has been used.   Where the body shape can be locally approximated by a straight line a cartesian grid has been used.

The local values ρ and p at the forward stagnation point of the NACA-0012 aerofoil are given by equations (49) and (50).   The far-field boundary conditions for both aerofoils have been obtained by applying a Prandtl-Glauert transformation to the x-coordinate and applying thin-aerofoil theory to the distorted body. This is described in Appendix I.

5.1 6% circular-arc aerofoil

Solutions to the flow about a 6% circular-arc aerofoil have been obtained for various free-stream Mach numbers.   All the results presented in figures 7 to 10 have been obtained with 102 elements and 868 nodal unknowns spanning the flow-field.

The surface pressure distribution for a free-stream Mach number of 0.71 is shown in figure 7.   Also shown in figure 7 are experimental results due to Knechtel(ref.22).   Knechtel obtained pressure distributions for a completely smooth aerofoil for which the boundary layer would have been laminar at least to the 50% chord point.   By introducing roughness just aft of the leading edge Knechtel also obtained results for which the boundary layer was turbulent throughout.   An examination of figure 7 indicates that the finite element solution is in good agreement with the experimental solution obtained with a smooth aerofoil.   The shape of the pressure distribution is slightly different particularly close to the leading and trailing edges.   This may be due to the courseness of the grid at the body surface used to obtain the computational solution.   A consideration of the experimental accuracy suggests that in an area of rapidly changing pressure such differences indicated may not be significant.

The surface pressure distribution for a free-stream Mach number of 0.82 is shown in figure 8.   Also included in figure 8 are experimental results due to Knechtel(ref.22).   The experimental results were obtained with a smooth

aerofoil.   As in figure 7 the agreement shown in figure 8 is good.   For the
results shown in figures 7 and 8 the flow-field is everywhere subsonic.

The results shown in figures 9 and 10 have been obtained at a free-stream
Mach number of 0.88 for which the surface flow is just sonic at the thickest
part of the aerofoil.   The pressure distribution for this case is shown in
figure 9.   Experimental results at M_∞ = 0.88 were not obtained by Knechtel

(ref.22), although an interpolation of the results that are available
suggests that the negative pressure coefficient at the 50% chord point is
larger for the experimental results than it is for the computational results
shown in figure 9.   It is likely that the displacement thickness effect has
caused some supersonic flow and this has increased the suction peak.   The
corresponding surface Mach number distribution is shown in figure 10 and the
local Mach number at the 50% chord point can be seen to be sonic.

5.2 NACA-0012 aerofoil

Computational solutions have been obtained for the flow about a NACA-0012
aerofoil at free-stream Mach numbers of 0.4 and 0.72.   The finite element
solution for the free-stream Mach number of 0.4 has been obtained with a least-
squares formulation and 88 elements and 767 nodal unknowns spanning the flow-
field.   This solution is shown in figure 11.   Also shown in figure 11 are
experimental results due to Amick(ref.23) and some computational results,
using a finite difference method, due to Emmons(ref.24).

The finite element solutions have simulated an aerofoil in an unconstrained
free-stream.   In contrast the experimental results of Amick have not been
corrected for the influence of the wind-tunnel walls and the computational
results of Emmons have deliberately allowed for the presence of the wind-
tunnel walls.   The discussion in reference 24 suggests the experimental
results of Amick would produce a maximum negative pressure coefficient
approximately 4 to 5% less if the aerofoil were in an unconstrained free-stream.

It is apparent that the occurrence of the stagnation point in the flow-
field and the consequent acceleration of the flow past the nose of the aero-
foil causes a very rapid change in the values of the dependent variables in
the nose region.   To obtain accurate solutions this situation requires small
elements in that region and, if the computation time is to be kept within
reasonable bounds requires large elements elsewhere(figure 6).   The automatic
mesh generation scheme is the same as that used and described in reference 9
and the above requirements have only been partially achieved.   Nevertheless
the agreement with the experimental results shown in figure 11 is good
particularly away from the nose region.

A solution obtained for the flow about a NACA-0012 aerofoil at a free-
stream Mach number of 0.72 is presented in figure 12.   These results were
obtained with the least-squares formulation and 96 elements and 837 nodal
unknowns spanning the flow-field.   Computational result; for this problem
have been obtained by Lock(ref.25) using the method of Sells(ref.26).   Lock
considers that Sells' method is capable of giving results that are accurate
to 1% of the maximum perturbation velocity.   A feature of Sells' method is
the mapping of the flow-field onto the interior of a unit circle.   This
avoids the problem of applying the far-field boundary condition at a finite
distance from the body.   The solution obtained by Sells' method is shown
in figure 12.   An examination of figure 12 indicates that the finite element
solution for the pressure coefficient underpredicts Sells' solution
particularly in the nose region.   This may be due to not applying the far-
field boundary conditions sufficiently far from the body.   A more likely
cause is the courseness of the grid in a region where large gradients are
occurring.

6. COMPARISON OF THE GALERKIN AND LEAST-SQUARES FORMULATIONS

The Galerkin finite element formulation has been used frequently to find the numerical solution to flow problems.   However, most previous applications of the Galerkin formulation have been to the full Navier-Stokes equations in incompressible form.   In such a situation the viscous terms in the governing equations play a stabilising role in both the physical and numerical sense.   Viscosity plays no role in the present problem unless artificially introduced (Section 3.3). Most previous finite element solutions of the present problem have been based on a variational formulation which leads to a stiffness matrix that is positive definite.

The application of a Galerkin finite element formulation to the present problem has led to algebraic governing equations that are algebraicly simple, economical to create and relatively sparse.   In fact the derivation of the coefficients a_{ij}, b_{ij}, equation (24), in the algebraic equations is precisely the same as that for the application of the Galerkin formulation to incompressible, inviscid flow (ref.9).

A problem with the Galerkin formulation arises in relation to finding a suitable iterative scheme for solving the nonlinear algebraic governing equations. In the application of the Galerkin finite element method to slow viscous flow Newton's method has been used with considerable success.   Since Newton's method is completely general it should be effective in the present situation.   The first difficulty that occurred in implementing Newton's method was that the Jacobian was singular due to the symmetry about the y-axis.   To overcome this problem it was necessary to introduce special equations on the y-axis and on the body.   A second difficulty with Newton's method, and it may be related to the first difficulty, was that it failed to converge for large numbers of nodal unknowns even when starting from a solution close to a previously converged solution.

In contrast the least-squares finite element formulation produced algebraic equations that were more complex, required more computation time to form and were less sparse than those produced by the Galerkin formulation.   However, because of the positive definite nature of the stiffness matrix the iterative technique for solving the algebraic governing equations produced no convergence problems. At intermediate stages of the iterative process the solution was quite smooth which was in marked contrast to that produced by the Galerkin formulation at intermediate stages.

It seems reasonable to conclude that since the current problem is dominated by the non-linear convective terms the choice of the iterative scheme for solving the non-linear algebraic governing equations becomes crucial.   Thus any finite element formulation that leads to a positive definite stiffness matrix is likely to have a considerable advantage over any formulation that does not.

7. CONCLUSIONS

The main conclusion of this report is that the least-squares finite element formulation has been very effective in obtaining solutions to compressible, inviscid flow and the Galerkin formulation has not.   Additional conclusions are that the use of a primitive variable formulation results in very accurate solutions and that the combination of using the conservation form of the governing equations and representing groups of variables rather than single variables leads to a sparser stiffness matrix and hence a more economical solution.   In contrast to the treatment of slow, viscous flow, the most efficient finite element solution of the present problem is obtained if each group of variables in the governing equations is represented by shape functions of the same order.

NOTATION

F, G	vectors of groups of terms appearing in the equations of motion
I	unit matrix
J	Jacobian
L	shape function
M	Mach number, shape function
M_T	Mach number at body surface
N	shape function
R	equation residual
U_∞	free-stream velocity
W	vector of nodal unknowns
X	vector of groups of terms appearing in the continuity equation
Y	vector of groups of terms appearing in the momentum equations
a	sound speed
a_{ij}, b_{ij}, c_{ij}, s_{ij}	algebraic coefficients in the governing equations (Galerkin formulation)
N	order of shape function, number of nodes
p	pressure
$\overline{q}_i$	vector of nodal unknowns
q_T	tangential velocity at body surface
r_{ij}, s_{ij}, t_{ij}, x_{ij}, y_{ij}, z_{ij}	algebraic groups in the governing equations (least-squares formulation)
s	coordinate along the body surface
t	time
u	velocity component in the x direction
v	velocity component in the y direction
x,y	cartesian coordinates
α	parameter controlling stabilising terms in the equations of motion; parameter controlling relative influence of the residuals

γ specific heat ratio; correction to the Jacobian

δ correction vector

λ scalar in Newton's method

ρ density

φ velocity potential

Subscripts

fs   free-stream

nd   nondimensional

sp   stagnation point

ν iteration step

∞ conditions in the free-stream

-                        nodal value

o   differentiation with respect to time

REFERENCES

No.	Author	Title
1	de Vries, G. and Norrie, D.H.	"The Application of the Finite Element Technique to Potential Flow Problems". Trans. A.S.M.E., Series E, Journal of Applied Mechanics, Vol.38, pp 798 to 802, 1971
2	Periaux, J.	"Three Dimensional Analysis of Compressible Potential Flows". International Journal for Numerical Methods in Engineering, Vol.9, No.4, pp 775 to 833, 1975
3	Labrujere, Th.E. and van der Vooren, J.	"Finite Element Calculation of Axisymmetric, Subcritical, Compressible Flow". TR-74162U, National Aerospace Laboratory, The Netherlands, 1974
4	Chan, S.T.K., Brashears, M.R. and Young, V.Y.C.	"Finite Element Analysis of Transonic Flow by the Method of Weighted Residuals". AIAA 13th Aerospace Science Meeting, Pasadena, January 1975
5	Peyret, R. and Viviand, H.	"Computation of Viscous Compressible Flows Based on the Navier-Stokes Equations". AGARDOGRAPH No. 212, 1975
6	Fletcher, C.A.J. and Holt, M.	"An Improvement to the Method of Integral Relations". Journal of Computational Physics, Vol.18, No.2, pp 154 to 164, 1975
7	Fletcher, C.A.J. and Holt, M.	"Supersonic Viscous Flow over Cones at Large Angles of Attack". Journal of Fluid Mechanics, Vol.74, Part 3, pp 561 to 591, 1976
8	Hood, P. and Taylor, C.	"Navier-Stokes Equations Using Mixed Interpolation". in "Finite Element Methods in Flow Problems", ed. J.T. Oden et al., University of Alabama Press, 1974
9	Fletcher, C.A.J.	"The Application of the Finite Element Method to Two-Dimensional Inviscid Flow". WRE-TN-1606 (WR&D), May 1976
10	Fletcher, C.A.J.	"The Galerkin Method: An Introduction". in "Numerical Simulation of Fluid Motion", ed. B.J. Noye, North-Holland, 1977
11	Zienkiewicz, O.C., Owen, D.R.J. and Lee, K.N.	"Least-Squares Finite Element for Elasto-Plastic Problems. Use of 'Reduced' Integration". International Journal for Numerical Methods in Engineering, Vol.8, pp 341 to 358, 1974

No.	Author	Title
12	Rheinboldt, W.C.	"On the Solution of Large, Sparse Sets of Non-Linear Equations". University of Maryland, TR-324, 1974
13	Isaacson, E. and Keller, H.B.	"Analysis of Numerical Methods". Wiley, New York, 1966
14	Ortega, J.M. and Rheinboldt, W.C.	"Iterative Solutions of Non-Linear Equations in Several Variables". Academic Press, New York, 1970
15	Fletcher, C.A.J.	"POWIT: A Program for Solving Non-Linear Algebraic Equations". WRE-TN-1431 (WR&D), June 1975
16	Gear, C.W.	"The Automatic Integration of Ordinary Differential Equations". Communications of A.C.M., Vol.14, pp 176 to 179, 1971
17	Jones, D.J., South, J.C. and Klunker, E.B.	"On the Numerical Solution of Elliptic Partial Differential Equations by the Method of Lines". Journal of Computational Physics, Vol.9, pp 496 to 527, 1972
18	Greenspan, D. and Jain, P.C.	"Application of a Method for Approximating Extremals of Functionals to Compressible Subsonic Fluid Flows". Journal of Mathematical Analysis and Applications, Vol.18 pp 85 to 111, 1967
19	Imai, I.	"On the Flow of a Compressible Fluid Past a Circular Cylinder". Proceedings of the Physics and Mathematics Society of Japan, Series 3, Vol.23, pp 180 to 193, 1941
20	Lush, P.E. and Cherry, T.M.	"The Variational Method in Hydrodynamics". Journal of Mechanics and Applied Mathematics, Vol.9, pp 6 to 21, 1956
21	Belotserkovskii, O.M. and Chushkin, P.K.	"The Numerical Solution of Problems in Gas Dynamics". in "Basic Developments in Fluid Dynamics". (ed. M. Holt), Vol.1, Academic Press, New York pp 89 to 126, 1965
22	Knechtel, E.D.	"Experimental Investigation at Transonic Speeds of Pressure Distributions over Wedge and Circular-Arc Airfoil Sections and Evaluations of Perforated Wall Interference". NASA TN-D-15, 1959
23	Amick, J.L.	"Comparison of the Experimental Pressure Distribution on an NACA-0012 Profile at High Speeds with that Calculated by the Relaxation Method". NACA TN-2174, 1950

No.	Author	Title
24	Emmons, H.W.	"Flow of a Compressible Fluid Past a Symmetrical Airfoil in a Wind Tunnel and in Free Air". NACA TN-1746, 1948
25	Lock, R.C.	"Test Cases for Numerical Methods in Two-Dimensional Transonic Flows". AGARD Report No. 575, 1970
26	Sells, C.C.L.	"Plane Sub-Critical Flow past a Lifting Aerofoil". R.A.E. TR-67146, 1967

APPENDIX I

FAR-FIELD BOUNDARY CONDITIONS

For most of the results presented in this report the far-field boundary conditions have been determined by assuming that the body introduces a disturbance into the flow. Since the disturbance in the far-field is small it is appropriate to introduce a disturbance potential, φ which perturbs a uniform free-stream, i.e.,

$$\Phi = U_\infty \cdot x + \varphi. \tag{I.1}$$

For subcritical flow φ is governed by

$$\frac{1}{(1 - M_\infty^2)} \cdot \frac{\partial^2 \varphi}{\partial x^2} + \frac{\partial^2 \varphi}{\partial y^2} = 0. \tag{I.2}$$

A new coordinate $\overline{x} = (1 - M_\infty^2)^{\frac{1}{2}} \cdot x$ is introduced and the governing equation (I.2) reduces to Laplace's equation

$$\frac{\partial^2 \varphi}{\partial \overline{x}^2} + \frac{\partial^2 \varphi}{\partial y^2} = 0. \tag{I.3}$$

For the flow about circular and elliptic cylinders complex variable solutions (which satisfy equation (I.3)) are introduced and the far-field velocity components calculated.

For the flow about aerofoils a continuous source distribution is introduced along the chord line of the aerofoil. The source strength is proportional to the local distorted body slope, $dy/d\overline{x}$. The source distribution satisfies equation (I.3). The velocities induced by the source distribution are

$$u_{fs} - i \cdot v_{fs} = \frac{2}{\pi} \int_0^1 \left[\frac{dy/d\overline{x}(s)}{(\overline{x}_{f.s.} + i \cdot y_{fs}) - s} \right] ds. \tag{I.4}$$

s is the non-dimensional distance along the aerofoil chord. The integration in equation (I.4) has been performed numerically by dividing up the aerofoil chord into the same finite elements as are used in the body of the report, and summing the contributions from each element. Gauss quadrature and an isoparametric formulation are utilised to perform the integration over each element.

Once the far-field velocity components have been obtained the corresponding density and pressure are given by

$$\rho_{fs} = \left\{ 1 + \frac{\gamma - 1}{2} M_\infty^2 \cdot \left[1 - (u_{fs}^2 + v_{fs}^2) \right] \right\}^{\frac{1}{\gamma - 1}} \tag{I.5}$$

and

$$P_{fs} = (\rho_{fs}^\gamma - 1)/\gamma M_\infty^2. \tag{I.6}$$

The above linearised solutions have also been used to provide starting data throughout the domain.

APPENDIX II

DERIVATION OF THE ALGEBRAIC EQUATIONS OBTAINED
FROM THE LEAST-SQUARES FORMULATION

After application of the least-squares finite element formulation to equations (4) to (6) the following algebraic equations are obtained:

$$S_i^{(m)} = \sum_j \left\{ r_j^{(m)} \cdot (\overline{\rho u})_j + s_{ij}^{(m)} \cdot (\overline{\rho v})_j + t_{ij}^{(m)} \cdot (\overline{\rho u^2})_j + x_{ij}^{(m)} \cdot (\overline{\rho uv})_j + y_{ij}^{(m)} \cdot \right.$$

$$\left. (\overline{\rho v^2})_j + z_{ij}^{(m)} \cdot \overline{p}_j \right\} = 0$$

$$m = 1,3; \quad i = 1,n. \tag{II.1}$$

In equations (II.1) the actual expressions for r_{ij} etc. depend on which relationship is used to link p to the other variables. If p is related to the density by the isentropic equation

$$1 + \gamma \cdot M_\infty^2 \, p = \rho^\gamma \tag{II.2}$$

then the following expressions are obtained

$$r_{ij}^{(1)} = a_c \cdot a_{ij} \cdot \overline{\rho}_i$$

$$s_{ij}^{(1)} = a_c \cdot c_{ij} \cdot \overline{\rho}_i$$

$$t_{ij}^{(1)} = a_x \cdot \{2 \cdot a_{ij} \cdot (\overline{\rho u})_i + d_{ij} \cdot (\overline{\rho v})_i\} \tag{II.3}$$

$$x_{ij}^{(1)} = a_y \cdot c_{ij} \cdot (\overline{\rho v})_i$$

$$y_{ij}^{(1)} = a_x \{2 \cdot c_{ij} \cdot (\overline{\rho u})_i + b_{ij} \cdot (\overline{\rho v})_i\} + a_y \cdot a_{ij} \cdot (\overline{\rho v})_i$$

$$z_{ij}^{(1)} = a_x \{2 \cdot a_{ij} \cdot (\overline{\rho u})_i + d_{ij} \cdot (\overline{\rho v})_i\} + a_y \cdot c_{ij} \cdot (\overline{\rho v})_i.$$

$$r_{ij}^{(2)} = a_c \cdot d_{ij} \cdot \bar{\rho}_i$$

$$s_{ij}^{(2)} = a_c \cdot b_{ij} \cdot \bar{\rho}_i$$

$$t_{ij}^{(2)} = a_x \cdot d_{ij} \cdot (\overline{\rho u})_i$$

$$x_{ij}^{(2)} = a_y \cdot \{c_{ij} \cdot (\overline{\rho u})_i + 2 \cdot b_{ij} \cdot (\overline{\rho v})_i\}$$ (II.4)

$$y_{ij}^{(2)} = a_x \cdot b_{ij} \cdot (\overline{\rho u})_i + a_y \cdot \{a_{ij} \cdot (\overline{\rho u})_i + 2 \cdot d_{ij} \cdot (\overline{\rho v})_i\}$$

$$z_{ij}^{(2)} = a_x \cdot d_{ij} \cdot (\overline{\rho u})_i + a_y \cdot \{c_{ij} \cdot (\overline{\rho u})_i + 2 \cdot b_{ij} \cdot (\overline{\rho v})_i\} .$$

$$r_{ij}^{(3)} = 0$$

$$s_{ij}^{(3)} = 0$$

$$t_{ij}^{(3)} = a_x \cdot \left\{ a_{ij} \cdot \left[\frac{\bar{\rho}_i^{-\gamma+1}}{M_\infty^2} - (\overline{\rho u})_i^2 \right] - d_{ij} \cdot (\overline{\rho u})_i \cdot (\overline{\rho v})_i \right\}$$

$$x_{ij}^{(3)} = a_y \cdot \left\{ b_{ij} \cdot \left[\frac{\bar{\rho}_i^{-\gamma+1}}{M_\infty^2} - (\overline{\rho u})_i^2 \right] - c_{ij} \cdot (\overline{\rho u})_i \cdot (\overline{\rho v})_i \right\}$$ (II.5)

$$y_{ij}^{(3)} = a_x \cdot \left\{ c_{ij} \cdot \left[\frac{\bar{\rho}_i^{-\gamma+1}}{M_\infty^2} - (\overline{\rho u})_i^2 \right] - b_{ij} \cdot (\overline{\rho u})_i \cdot (\overline{\rho v})_i \right\}$$

$$+ a_y \left\{ d_{ij} \cdot \left[\frac{\bar{\rho}_i^{-\gamma+1}}{M_\infty^2} - (\overline{\rho v})_i^2 \right] - a_{ij} \cdot (\overline{\rho u})_i \cdot (\overline{\rho v})_i \right\}$$

$$z_{ij}^{(3)} = a_x \left\{ a_{ij} \cdot \left[\frac{\bar{\rho}_i^{-\gamma+1}}{M_\infty^2} - (\overline{\rho u})_i^2 \right] - d_{ij} \cdot (\overline{\rho u})_i \cdot (\overline{\rho v})_i \right\}$$

$$+ a_y \left\{ b_{ij} \cdot \left[\frac{\bar{\rho}_i^{-\gamma+1}}{M_\infty^2} - (\overline{\rho v})_i^2 \right] - c_{ij} \cdot (\overline{\rho u})_i \cdot (\overline{\rho v})_i \right\} .$$

If p is related to the other variables through the energy equation

$$1 + \gamma \cdot M_\infty^2 \cdot p = \rho \cdot \left\{ 1 + \frac{\gamma - 1}{2} \cdot M_\infty^2 \left[1 - (u^2 + v^2) \right] \right\} . \qquad (II.6)$$

the following expressions for $r_{ij}^{(m)}$ etc. are obtained

$$r_{ij}^{(1)} = a_c \cdot a_{ij} \cdot \overline{\rho}_i$$

$$s_{ij}^{(1)} = a_c \cdot c_{ij} \cdot \overline{\rho}_i$$

$$t_{ij}^{(1)} = a_x \cdot \left\{ \left(\frac{\gamma + 1}{\gamma} \right) \cdot a_{ij} \cdot (\overline{\rho u})_i + d_{ij} \cdot (\overline{\rho v})_i \right\}$$

$$x_{ij}^{(1)} = a_y \cdot \left\{ c_{ij} \cdot (\overline{\rho v})_i - \left(\frac{\gamma - 1}{\gamma} \right) \cdot b_{ij} \cdot (\overline{\rho u})_i \right\} \qquad (II.7)$$

$$y_{ij}^{(1)} = a_x \cdot \left\{ \left(\frac{\gamma + 1}{\gamma} \right) \cdot c_{ij} \cdot (\overline{\rho u})_i + b_{ij} \cdot (\overline{\rho v})_i \right\}$$

$$+ a_y \left\{ a_{ij} (\overline{\rho v})_i - \left(\frac{\gamma - 1}{\gamma} \right) \cdot d_{ij} \cdot (\overline{\rho u})_i \right\}$$

$$z_{ij}^{(1)} = a_x \left\{ \left(\frac{\gamma + 1}{\gamma} \right) \cdot a_{ij} \cdot (\overline{\rho u})_i + d_{ij} \cdot (\overline{\rho v})_i \right\}$$

$$+ a_y \left\{ c_{ij} \cdot (\overline{\rho v})_i - \left(\frac{\gamma - 1}{\gamma} \right) \cdot b_{ij} \cdot (\overline{\rho u})_i \right\} .$$

$$r_{ij}^{(2)} = a_c \cdot d_{ij} \cdot \overline{\rho}_i$$

$$s_{ij}^{(2)} = a_c \cdot b_{ij} \cdot \overline{\rho}_i$$

$$t_{ij}^{(2)} = a_x \cdot \left\{ d_{ij} \cdot (\overline{\rho u})_i - \left(\frac{\gamma - 1}{\gamma} \right) \cdot a_{ij} \cdot (\overline{\rho v})_i \right\}$$

$$x_{ij}^{(2)} = a_y \cdot \left\{ c_{ij} \cdot (\overline{\rho u})_i + \left(\frac{\gamma + 1}{\gamma} \right) \cdot b_{ij} \cdot (\overline{\rho v})_i \right\} \qquad (II.8)$$

$$y_{ij}^{(2)} = a_x \cdot \left\{ b_{ij} \cdot (\overline{\rho u})_i - \left(\frac{\gamma - 1}{\gamma} \right) \cdot c_{ij} \cdot (\overline{\rho v})_i \right\}$$

$$+ a_y \cdot \left\{ a_{ij} \cdot (\overline{\rho u})_i + \left(\frac{\gamma + 1}{\gamma} \right) \cdot d_{ij} \cdot (\overline{\rho v})_i \right\}$$

$$z_{ij}^{(2)} = a_x \cdot \{d_{ij} \cdot (\overline{\rho u})_i - (\frac{\gamma - 1}{\gamma}) \cdot a_{ij} \cdot (\overline{\rho v})_i\}$$

$$+ a_y \cdot \{c_{ij} \cdot (\overline{\rho u})_i + (\frac{\gamma + 1}{\gamma}) \cdot b_{ij} \cdot (\overline{\rho v})_i\} \ .$$

$$r_{ij}^{(3)} = 0$$

$$s_{ij}^{(3)} = 0$$

$$t_{ij}^{(3)} = a_x \cdot \left\{ a_{ij} \cdot \left[\overline{\rho}_i^2 \frac{\partial \overline{p}_i}{\partial \overline{\rho}_i} - (\overline{\rho u})_i^2 \right] - d_{ij} \cdot (\overline{\rho u})_i \cdot (\overline{\rho v})_i \right\}$$

$$x_{ij}^{(3)} = a_y \cdot \left\{ b_{ij} \cdot \left[\overline{\rho}_i^2 \frac{\partial \overline{p}_i}{\partial \overline{\rho}_i} - (\overline{\rho v})_i^2 \right] - c_{ij} \cdot (\overline{\rho u})_i \cdot (\overline{\rho v})_i \right\} \qquad (II.9)$$

$$y_{ij}^{(3)} = a_x \cdot \left\{ c_{ij} \cdot \left[\overline{\rho}_i^2 \frac{\partial \overline{p}_i}{\partial \overline{\rho}_i} - (\overline{\rho u})_i^2 \right] - b_{ij} \cdot (\overline{\rho u})_i \cdot (\overline{\rho v})_i \right\}$$

$$+ a_y \cdot \left\{ d_{ij} \cdot \left[\overline{\rho}_i^2 \frac{\partial \overline{p}_i}{\partial \overline{\rho}_i} - (\overline{\rho v})_i^2 \right] - a_{ij} \cdot (\overline{\rho u})_i \cdot (\overline{\rho v})_i \right\}$$

$$z_{ij}^{(3)} = a_x \cdot \left\{ a_{ij} \cdot \left[\overline{\rho}_i^2 \frac{\partial \overline{p}_i}{\partial \overline{\rho}_i} - (\overline{\rho u})_i^2 \right] - d_{ij} \cdot (\overline{\rho u})_i \cdot (\overline{\rho v})_i \right\}$$

$$+ a_y \cdot \left\{ b_{ij} \cdot \left[\overline{\rho}_i^2 \frac{\partial \overline{p}_i}{\partial \overline{\rho}_i} - (\overline{\rho v})_i^2 \right] - c_{ij} \cdot (\overline{\rho u})_i \cdot (\overline{\rho v})_i \right\} \ .$$

where

$$\frac{\partial \overline{p}_i}{\partial \rho_i} = \frac{1}{\gamma \cdot M_\infty^2} + (\frac{\gamma - 1}{2\gamma}) \cdot [1 + \overline{u}_i^2 + \overline{v}_i^2] \ . \qquad (II.10)$$
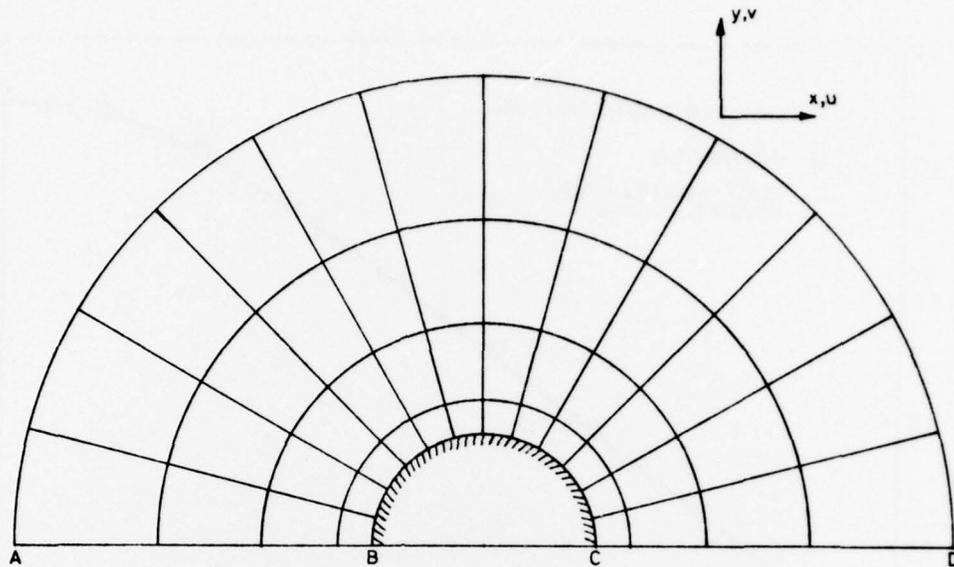
Figure 1. Flow-field geometry and schematic of grid for the circular cylinder
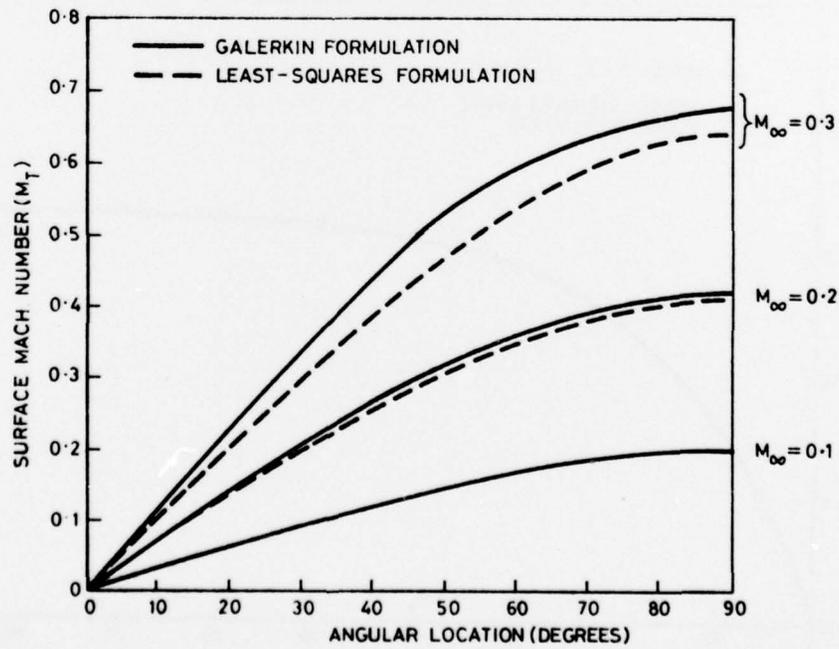
Figure 2. Surface Mach number variation for flow about a circular cylinder
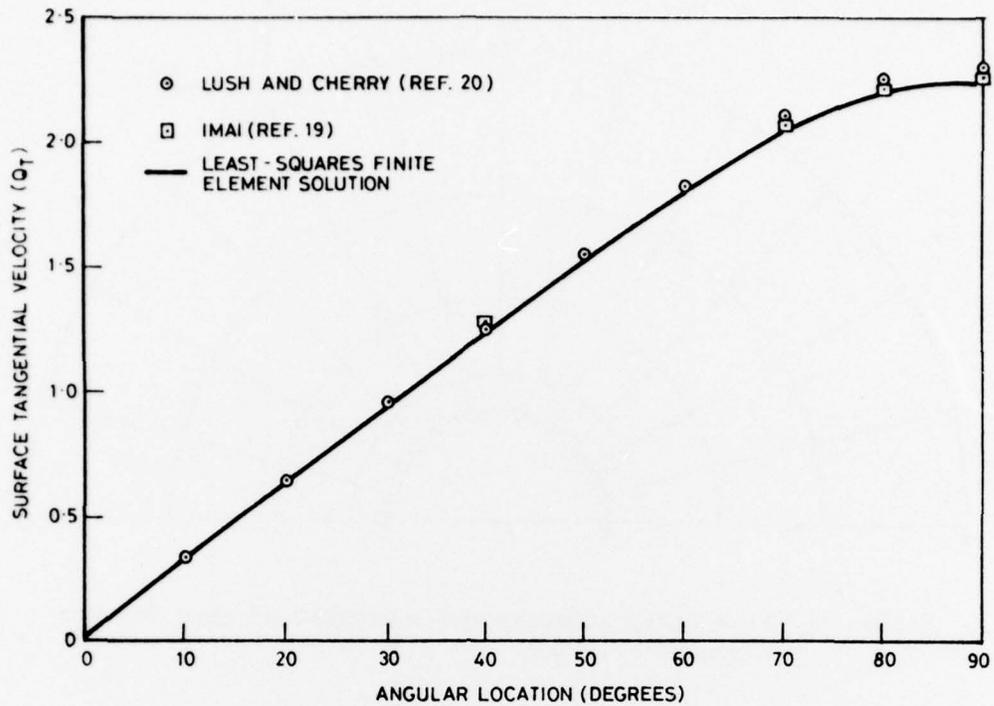
Figure 3. Surface velocity variation for the flow about a circular cylinder at $M_\infty = 0.40$
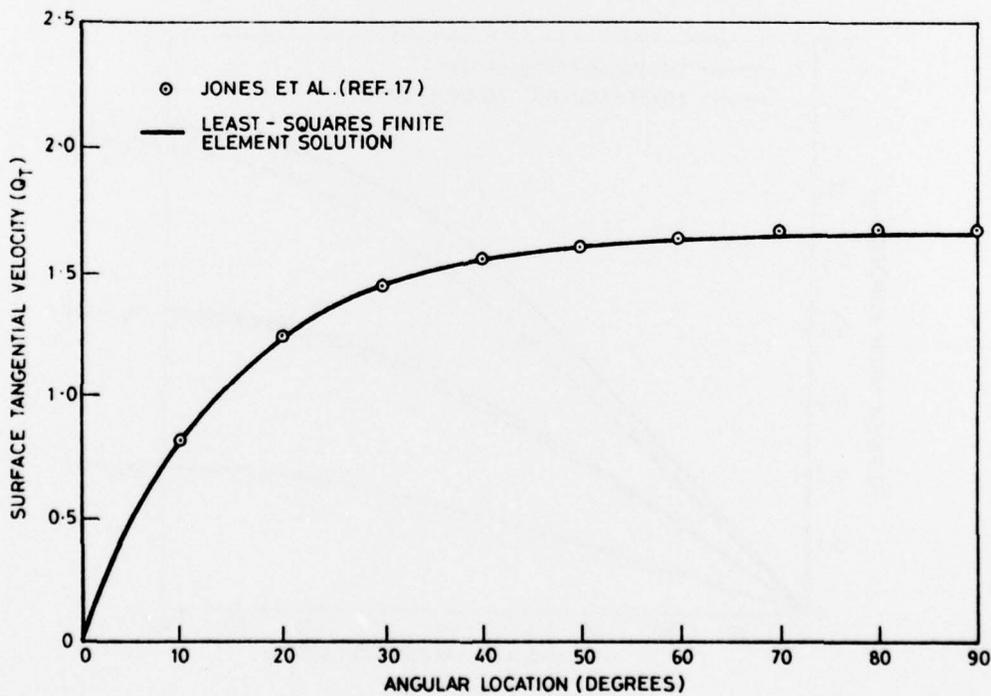
Figure 4. Surface velocity variation for the flow about a 2:1 elliptic cylinder at $M_\infty = 0.50$
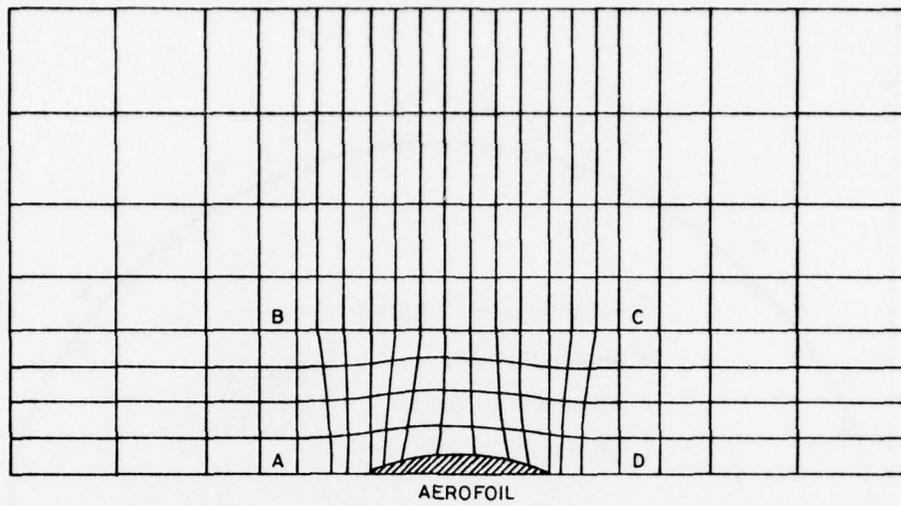
Figure 5. Schematic of the finite element grid used for the circular-arc aerofoil
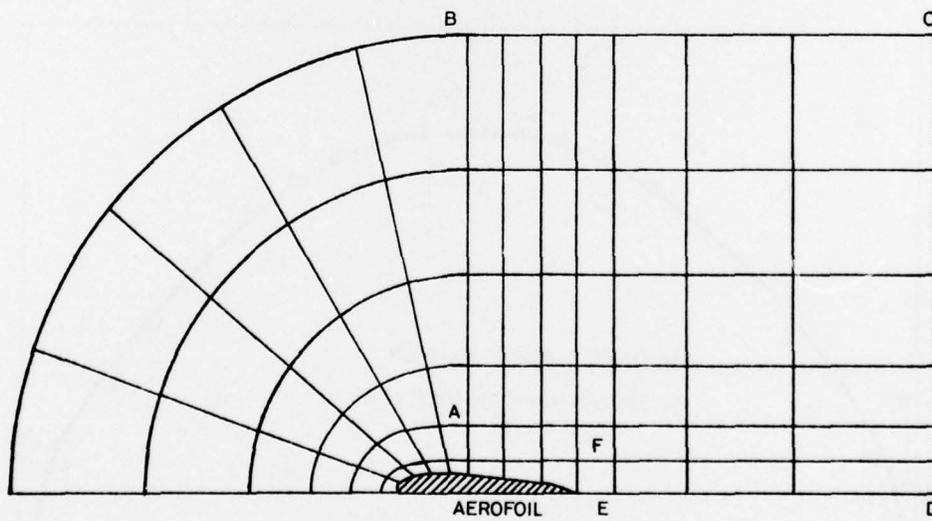
Figure 6. Schematic of the finite element grid used for the NACA-0012 aerofoil
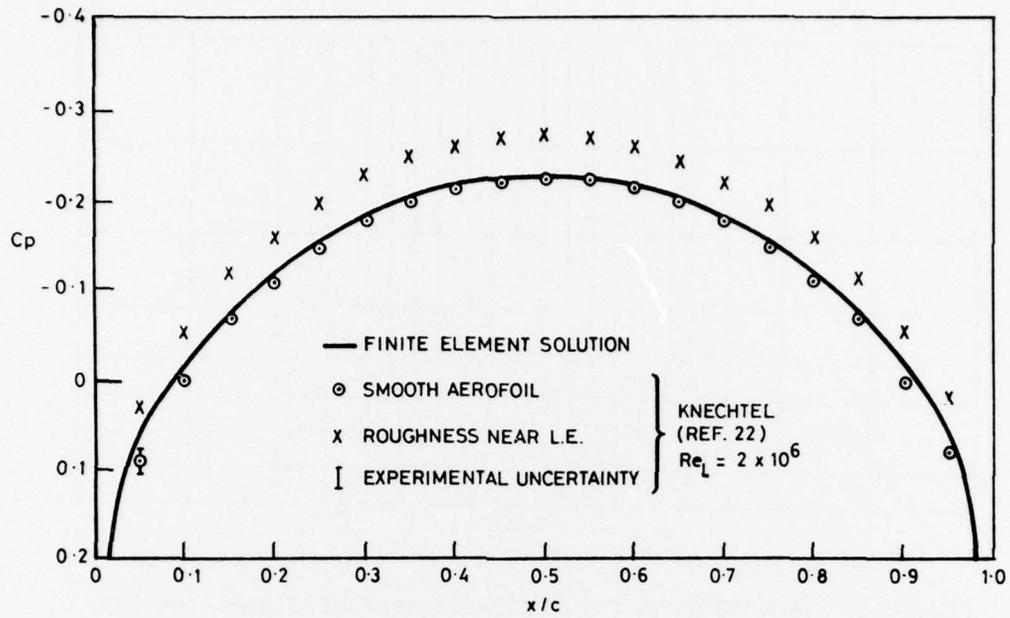
Figure 7. Pressure distribution on a 6% circular-arc aerofoil
at M_∞ = 0.71
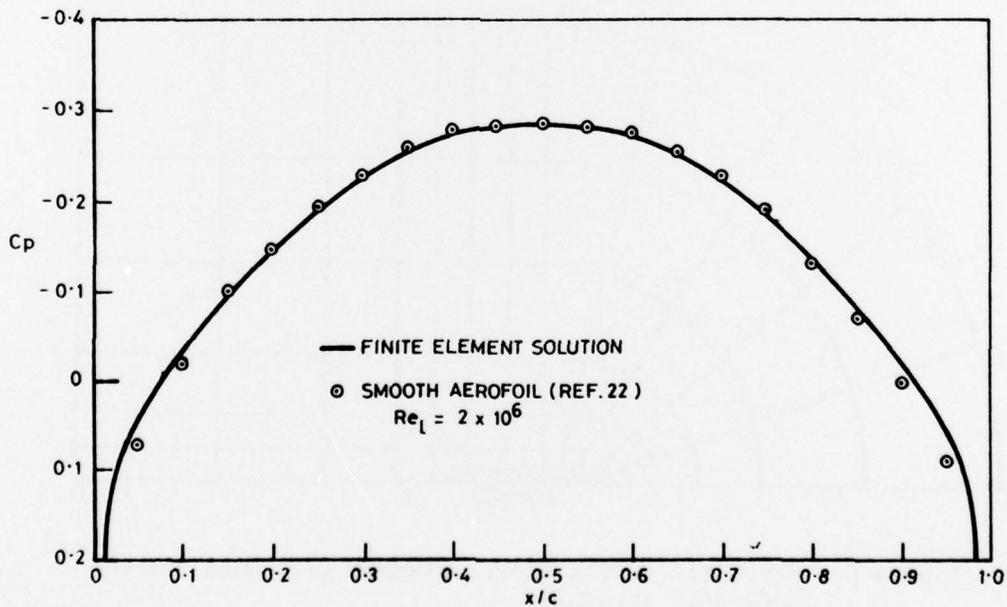
Figure 8. Pressure distribution on a 6% circular-arc aerofoil
at M_∞ = 0.82
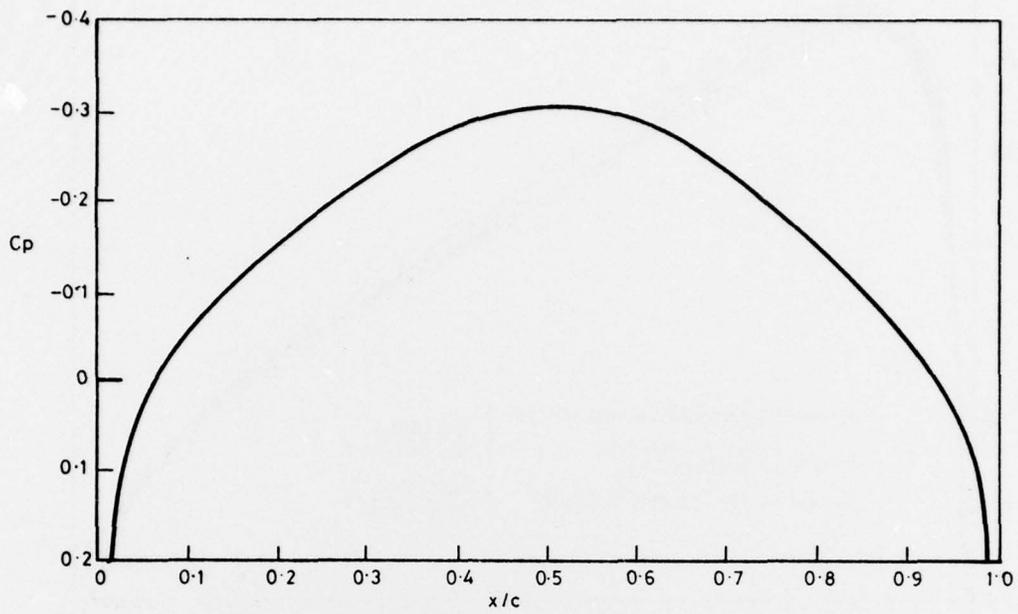
Figure 9.   Pressure distribution on a 6% circular-arc aerofoil
at $M_\infty = 0.88$
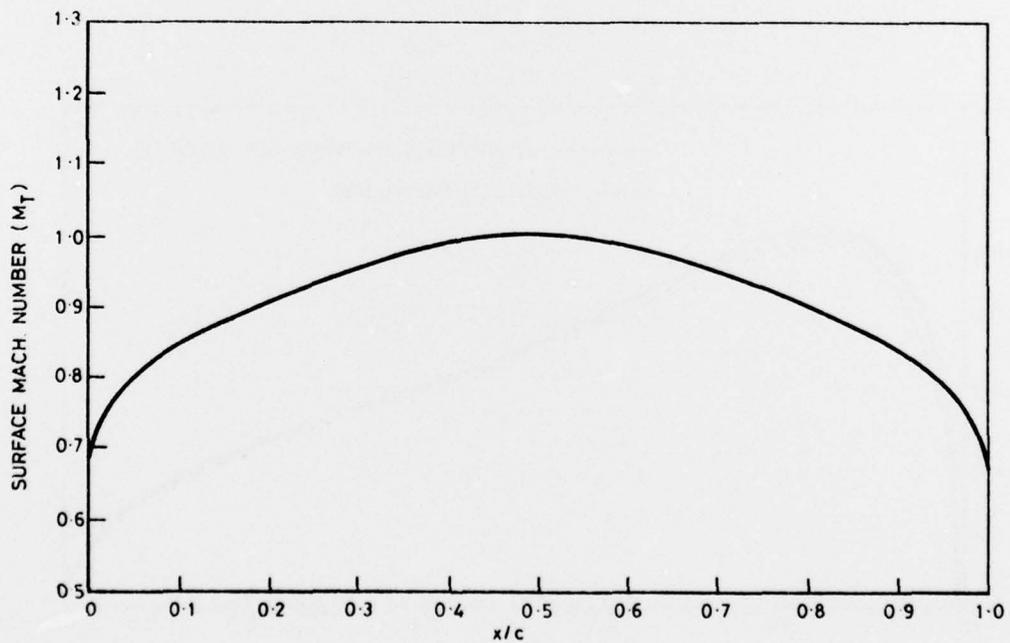
Figure 10.   Surface Mach number variation on a 6% circular-arc
aerofoil at $M_\infty = 0.88$
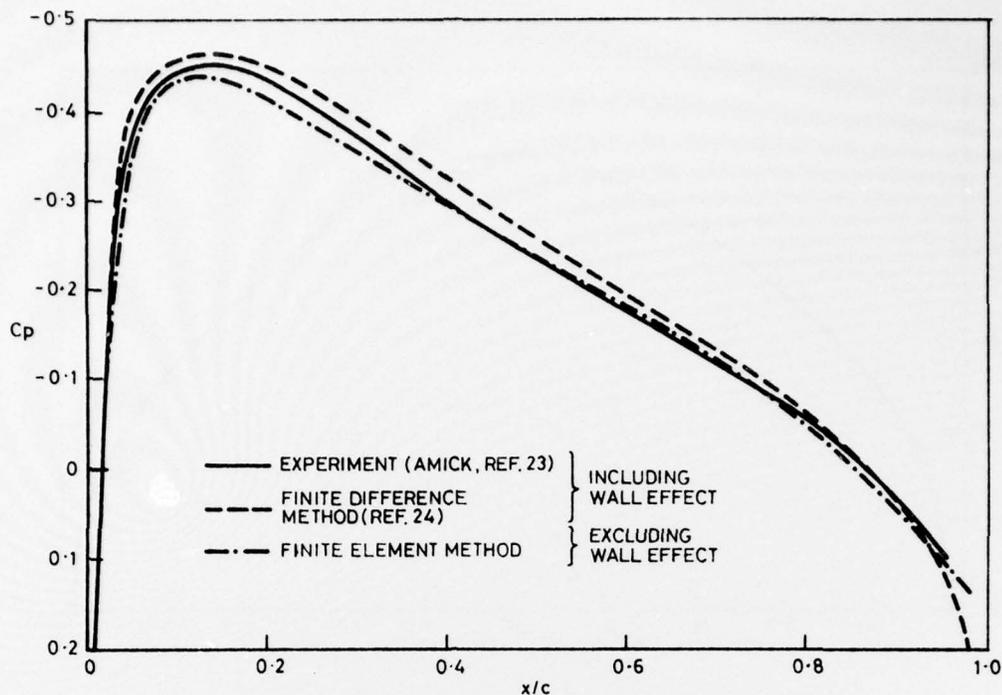
Figure 11.   Pressure distribution on a NACA-0012 aerofoil
at $M_\infty = 0.40$
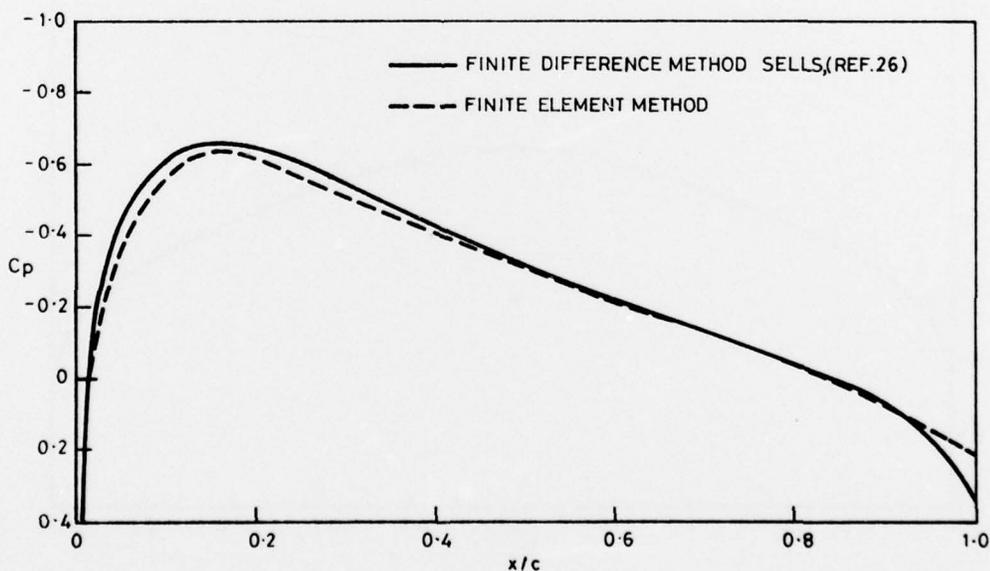
Figure 12.   Pressure distribution on a NACA-0012 aerofoil
at $M_\infty = 0.72$

DISTRIBUTION

EXTERNAL	Copy No.
In United Kingdom	
Defence Scientific and Technical Representative, London	1
Royal Aircraft Establishment	
Aero Department	2 - 3
Space Department	4
Weapons Department	5 - 6
Bedford	7
Library	8
R.A.R.D.E.	9
T.T.C.P., U.K. National Leader Panel W-2	10 - 13
Aeronautical Research Council	14 - 15
Aircraft Research Association (Bedford)	16
Secretary, C.A.A.R.C.	17
National Lending Library of Science and Technology	18
Library, Royal Aeronautical Society	19
Library, Cranfield Institute of Technology	20
Library, Imperial College, Department of Aeronautical Engineering	21
Queen Mary College, Department of Aeronautical Engineering	22
University of Bristol, Department of Aeronautical Engineering	23
University of Manchester, Department of Mechanics of Fluids	24
University of Southampton, Department of Aeronautics and Astronautics	25
Professor O.C. Zienkiewicz, Department of Civil Engineering, University College of Swansea	26
Professor J.R. Whiteman, Department of Mathematics, Brunel University	27
In United States of America	
Counsellor, Defence Science, Washington	28
Defence Research and Development Attache, Washington	29
Applied Physics Laboratory, Johns Hopkins University	30
Air Force Armament Testing Laboratory	31
Ballistics Research Laboratories	32
Edgewood Arsenal	33
Eglin Air Force Base	34
N.A.S.A.	35 - 38
Naval Surface Weapons Center	
Dahlgren	39
White Oak	40

Copy No.

Naval Weapons Center	41
Naval Ship Research and Development Center	42
Picatinny Arsenal	43
Redstone Arsenal	44
T.T.C.P. U.S. National Leader Panel W-2	45 - 48
Library, Wright-Patterson Air Force Base	49
Library, American Institute of Aeronautics and Astronautics	50
Pacific Technical Information Services, Northrop Institute of Technology	51
Applied Mechanics Reviews	52
Arnold Engineering Development Center	53
A.R.O. Incorporated	54
Library, Sandia Corporation	55
Library, The Boeing Company, Seattle	56
Library, Douglas Aircraft Company, Long Beach	57
Professor W.F. Ames, Department of Mechanics and Hydraulics, University of Iowa, Iowa	58
Professor A.J. Baker, Old Dominion University, Norfolk, Virginia	59
Professor B.A. Finlayson, Department of Chemical Engineering, University of Washington	60
Professor M. Holt, Department of Mechanical Engineering, University of California, Berkeley	61
Department of Mechanical Engineering Library, University of California, Berkeley	62
Library, Massachusetts Institute of Technology, Aeronautics Department	63
Professor G. Moretti, Department of Aeronautical Engineering, Polytechnic Institute of Brooklyn	64
Library, New York University, Courant Institute of Mathematical Science	65
Professor J.T. Oden, The University of Texax, Austin	66
Library, Princeton University, Department of Aeronautics	67
Library, Stanford University, Department of Aeronautics	68
Dr T. Taylor, Fluid Mechanics Department, Aerospace Corporation	69
Library, T.R.W. Systems	70
Library, United Aircraft Research Laboratories	71
Library, University of Maryland, Institute of Fluid Dynamics and Applied Maths	72

Copy No.

Copy No.

INTERNAL